Australian Government
Department of Defence
Defence Science and
Technology Organisation

# Probabilistic Model of a Floating Target Behaviour in Rough Seas

*Rada Pushakrova*[a]

**Maritime Division**
Defence Science and Technology Organisation

[a]University of Adelaide

DSTO-TN-1196

## ABSTRACT

This note presents the results from modelling of floating target visibility and wave cover in rough seas. Waves on the sea surface can hide a target from observer's view affecting aiming and ammunition effectiveness. The randomly moving sea surface was modelled using a double peaked wave spectrum. The moving sea surface model was used to estimate height of an object hidden by waves depending on angle of sight, wave direction, significant wave height, target speed and time. Based on this data wave cover frequency distributions were calculated. A possible method of using this data in naval gun performance analysis for armour-piercing, point detonation high explosive, and air burst rounds was suggested.

## RELEASE LIMITATION

*Approved for public release*

*Published by*

*Maritime Division*
*DSTO*
*Defence Science and Technology Organisation*
*PO Box 1500*
*Edinburgh South Australia 5111  Australia*

*Telephone:  1300 DEFENCE*
*Fax:  (08) 7389 6567*


*AR-015-679*
*July 2013*

**APPROVED FOR PUBLIC RELEASE**

# Probabilistic Model of a Floating Target Behaviour in Rough Seas

## Executive Summary

The research and simulation activities described in this technical note were conducted in 2012 in support of operations of the Royal Australian Navy (RAN). This technical note examines effect of sea waves on small surface target visibility. The developed model of the target behaviour and visibility provides an input to naval gun performance analysis and modelling.

Since target visibility for an observer and target cover from gun fire are mathematically the same problem, terms "target visibility" and "target cover" are used interchangeably in this report.

Real oceanographic data for the area of interest could not be obtained in time for this project; therefore, the Soares-Torsethaugen spectral model was used as a closest available approximation to oceanographic situation in the area of interest since it describes combined action of wind and swell with limited fetch in coastal water. The sea surface was modelled for significant wave heights of 1.25 m, 2.5 m, and 3.0 m, that is, for sea states 3, 4, and 4-5.

Finding the target cover height was considered as a two-dimensional geometrical problem; for simplicity, no consideration was given to change of actual cover along the target waterline or for the target pitch and roll (e.g. the bow is completely covered by waves and the stem is completely exposed).

The computer model of wave cover behaved as expected: increase of angle of sight caused decrease of wave cover, increase of wave height resulted in higher and longer cover. The wave cover data is presented in the report as 15 frequency distributions for wave heights of 1.25, 2.5 and 3 m and angles of sight of 0, 2, 4, 6, and 8 degrees.

Modelling the effect of wave cover on gun performance could be done by introducing the ammunition effectiveness coefficient derived from the wave cover height. The ammunition effectiveness coefficient for armour-piercing and point detonation high explosive rounds is equal to the ratio of exposed target area and the total target area. The air burst munitions require different treatment; the coefficient should be estimated depending on the individual fragment lethality, fragment density, and target cover by waves.

The future work in modelling of floating target behaviour in rough seas can be aimed at improving the weapon firing modelling and developing a fast but realistic method of sea cover modelling. A future weapon firing model should be able to change target vulnerable area and/or round lethality on the round-to-round base. Combined with ability to simulate a realistic wave cover as a time series would enhance the future weapon performance analysis capability.

# Contents

*This page is intentionally blank*

# List of Abbreviations

| | |
|---|---|
| **ABM** | Air-Bursting fragmenting Munition |
| **AP** | Armour-Piercing round |
| **JONSWAP** | Joint North Sea Wave Project |
| **OH** | Ochi-Hubble wave spectrum |
| **PD-HE** | Point-Detonation High-Explosive round |
| **PM** | Pierson–Moskowitz wave spectrum |
| **ST** | Soares–Torsethaugen wave spectrum |

*This page is intentionally blank*

# 1. Introduction

The research and simulation activities described in this technical note were conducted in 2012 in support of operations of the Royal Australian Navy (RAN). This technical note examines effect of sea waves on small surface target visibility. The developed model of the target behaviour and visibility provides an input to naval gun performance analysis and modelling.

Waves on the sea surface can hide a small surface target from the observer's view as illustrated in Figure 1. The Thor Heyerdahl's Kon-Tiki raft on the photo is not fully visible because it is partially obscured by waves.

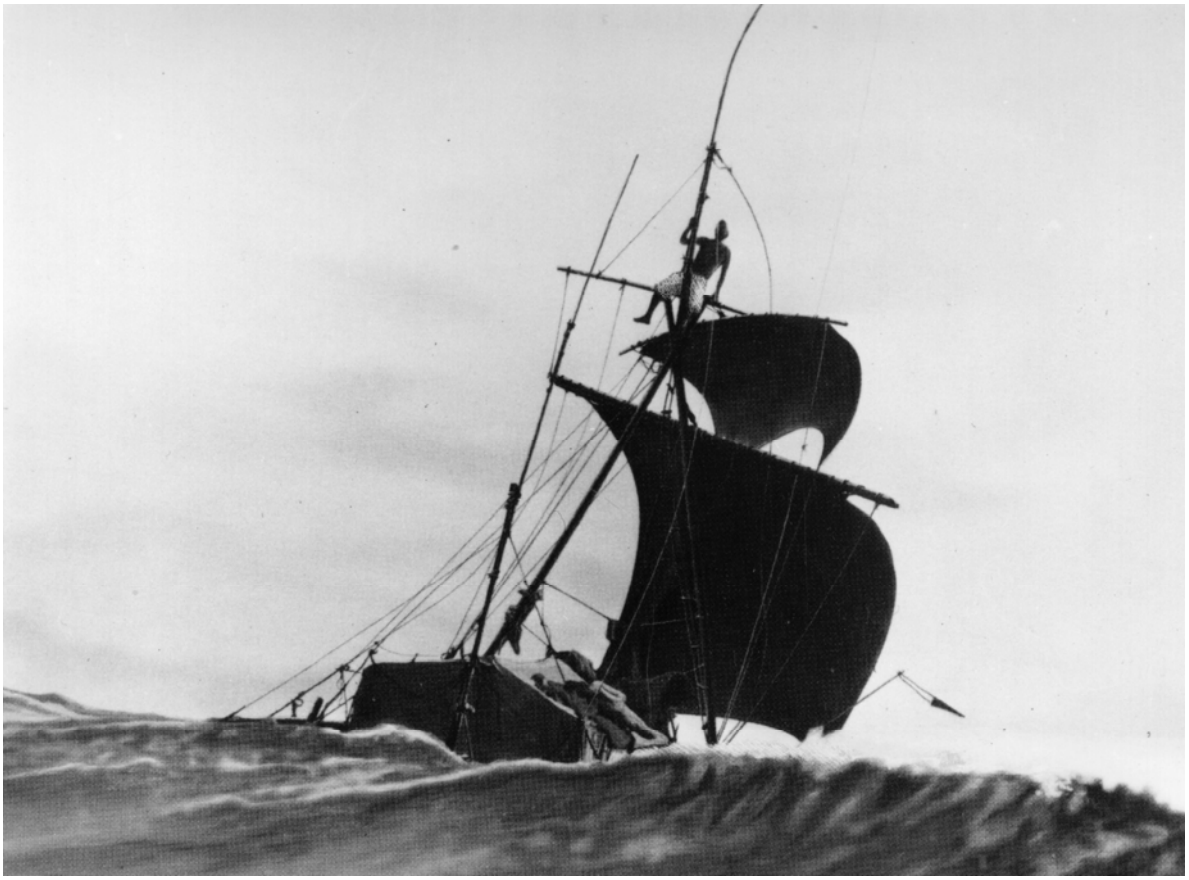

*Figure 1. The Kon-Tiki raft is fully hidden and the hut is partially hidden by sea waves. The image was sourced from the Internet [5].*

This effect influences naval gun performance in two ways: first, by affecting aiming, and second, by reducing ammunition effectiveness. If the target is hidden from the gunner's or sensor's field of view, the weapon cannot be aimed at the target. Even if the gunner succeeded in aiming and firing the weapon, by the time the round arrives the target might be in a trough and the round would hit the sea surface rather than the target.

Since target visibility for an observer and target cover from gun fire are mathematically the same problem (as it will be demonstrated later), terms "target visibility" and "target cover" are used interchangeably in this report.

The target cover problem is approached as follows. First, in Section 2 modelling of randomly moving sea surface is reviewed. Next, in Section 3 geometry of target cover by waves is studied. Results of calculation of target cover are presented in Section 4. There, ways of using the simulated data for a naval gun weapon performance analysis are discussed and a proposed method of use of wave cover frequency distribution in an existing weapon performance analysis methodology is outlined. Finally, in Section 5 the findings are summarised and ways of integrating the wave cover model into a future weapon performance analysis model are discussed. Detailed mathematical explanations of wave spectra and their use for modelling of evolution of a random sea surface are provided in Appendix A. The effect of sea state on ammunition performance is explained in detail in Appendix B. Finally, Appendix C contains tabulated frequency distributions of wave cover under various conditions.

# 2. Model of Sea Surface

## 2.1 Sea State and Significant Wave Height

Significant wave height is a commonly used characteristic of the sea surface, which is referred to as Seas in marine forecasts [7]. It is defined as an average height of the highest third of waves. The definition implies that there are waves higher than the given Seas, and over a reasonably long distance there is a good chance of finding a much higher wave, as shown in Table 1.

*Table 1. Sea state and wave heights*

| World Meteorological Organization sea state code | Significant wave height, m | The highest 10% of waves, m | The highest 1% of waves, m |
|---|---|---|---|
| 3 | 1.25 | > 1.6 | > 2.1 |
| 4 | 2.5 | > 3.2 | > 4.2 |
| 4-5 | 3.0 | > 3.8 | > 5.0 |

Therefore, evaluating wave effect on gun performance required building an appropriate sea surface model first, then solving the geometrical problem of target cover and calculating cover statistics, and finally applying this data to gun fire effectiveness problem. This process is schematically represented on Figure 2.

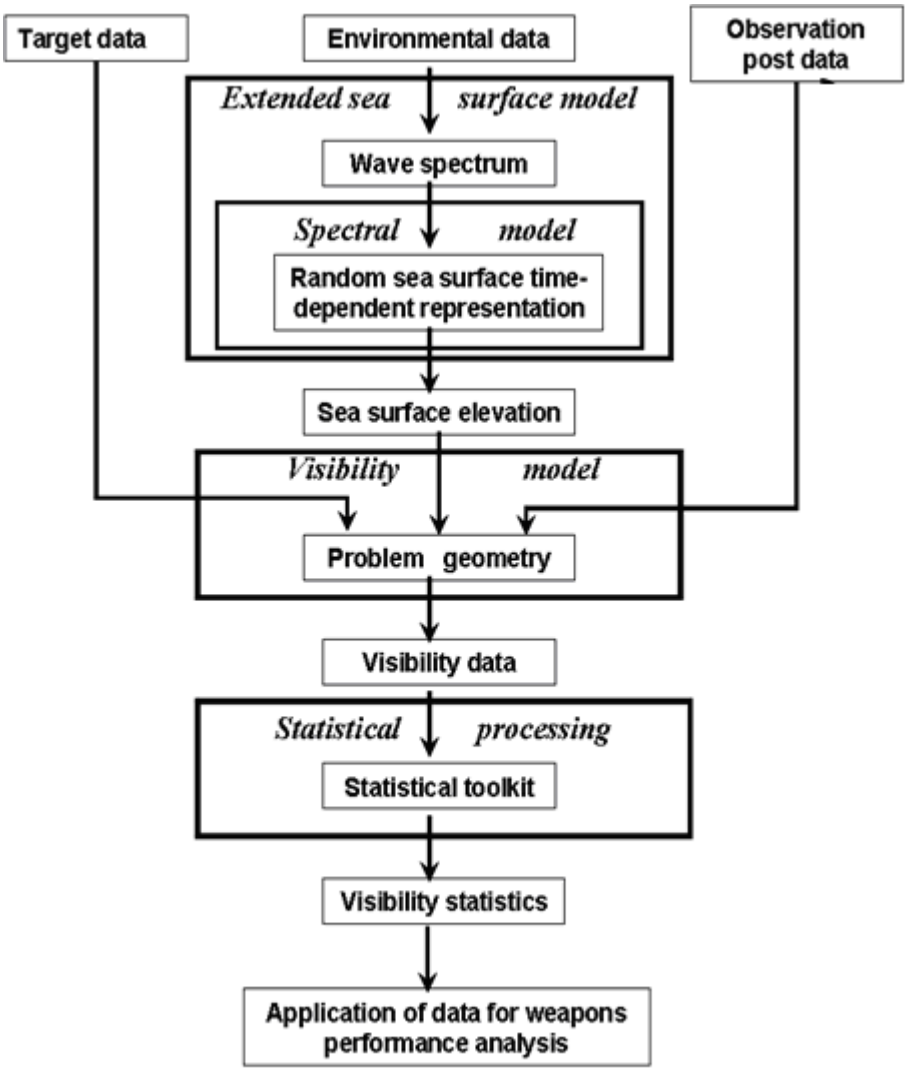


*Figure 2. Calculating target visibility or cover due to sea waves*

## 2.2 Target Cover by Sea Waves

Raw data on sea surface elevation is traditionally collected in some specific locations on the sea surface (stations) at some specific moments of time. Raw imagery or radar data collected from either aircraft of satellites require a special processing procedure to provide momentary sea surface height distribution over some area. Because of randomness of the sea surface, observation data should be accumulated over a long period of time.

A widely accepted approach to the random sea surface representation is based on works of Michael Longuet-Higgins dating back to the 1950s [6]. The rough sea surface is represented as a sum of harmonic (sinusoidal) waves with various frequencies, directions and random phase shift, as follows:

$$\zeta(x,y,t) = \sum_{n=1}^{N} a_n \cos(-k_{xn}x - k_{yn}y + \omega_n t + \varepsilon_n) \quad (1)$$

where:
$x$ and $y$ are the coordinates of the point on the sea surface, see Figure 3;
$t$ is time;
$a_n$ is the n-th harmonic wave amplitude;
$k_{xn}$ and $k_{yn}$ are projections of the n-th harmonic wave two-dimensional wave vector on $X$ and $Y$ axes respectively, see Figure 3;
$\omega_n$ is the n-th harmonic wave frequency – wave frequency;
$\varepsilon_n$ is the n-th harmonic wave random phase; these phases are uniformly distributed in the interval $(0, 2\pi)$.

From this representation it is possible to derive the energy distribution for all wave frequencies for a particular sea state using the Wiener-Khinchine theorem [8]. The energy distribution is commonly referred to as power spectrum or wave spectrum. The energy distribution does not depend on random phase shift of individual harmonic waves, and therefore the phase information is lost. For the reader's convenience the mathematical details are given in the Appendix A.

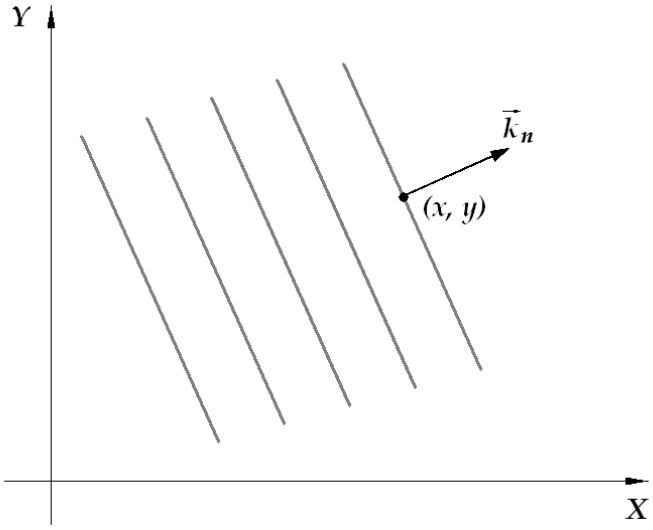


*Figure 3. The n-th harmonic wave*

The wave spectrum then can be used for the inverse process, namely to realistically simulate evolution of random sea surface for a particular sea state [1], [8]. It should be highlighted that this is not a reconstruction of the original sea surface shape because the phase information was irretrievably lost; the simulation builds a moving surface which has the same statistical properties as the original moving sea surface.

## 2.3 Wave Spectra

There are several empirical parametric models that describe sea wave energy distribution with wave frequency. The most common models are single peaked Pierson-Moskowitz (PM) [10] and JONSWAP spectra [3]. Both models were derived from experimental data from the Northern part of the Atlantic Ocean. PM model describes a fully developed sea surface with unlimited fetch. JONSWAP spectral model was derived from observation in the North Sea and is associated with developing seas in coastal waters with limited fetch.

Single peaked or unimodal spectra commonly describe sea surface that was developed under action of wind only. Also these spectra can be used to describe swell action alone, but not both wind and swell. However, the situation when the sea waves are result of combined action of both wind and swell action are much more realistic for naval gunnery applications. Such situations are modelled by double peaked spectra.

Commonly used doubly-peaked models are Ochi-Hubble (OH) [9] and Soares-Torsethaugen (ST) spectra [2] [13] [14]. Both models use similar approaches: they describe a bimodal spectrum as a superposition of two unimodal spectra. The Ochi-Hubble model uses two modified Pierson-Moskowitz spectra and the Soares-Torsethaugen model uses two modified JONSWAP spectra [11] [12].

An example of a doubly-peaked spectrum is shown on Figure 4. In this example the low-frequency component is swell with peak frequency 0.57 rad/s, which corresponds to the peak period of 11 s. The peak frequency for wing waves is 1.3 rad/s, which corresponds to the shorter peak period of 5 s. In this example swell waves have relatively lower energy then wind waves.

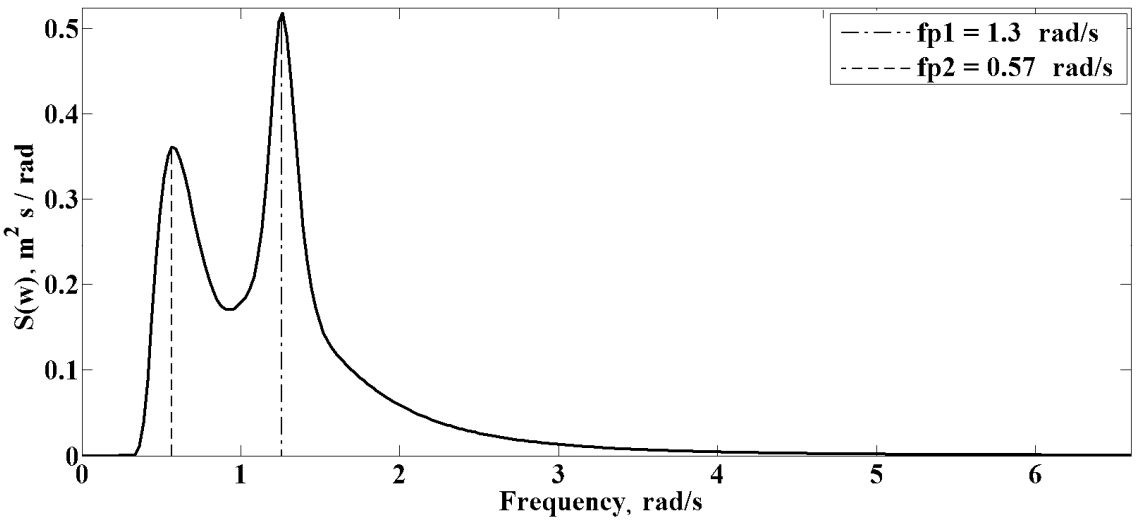


*Figure 4. Doubly-peaked (bimodal) wave spectrum*

The ST spectral model is likely to be a close approximation to the area of interest spectrum because this is the only model that describes combined action of wind and swell in coastal waters with limited fetch. Since all mentioned above models are geographically specific, suitability of the ST model for the geographic area of interest still has to be verified.

The ST model has two input parameters: significant wave height and main peak period. For our problem wave heights are limited to 3 m (sea state 4-5) due to practical reasons. Exact spectral data for the area of interest was unavailable at the time of writing of this note but from analysis of the data from similar areas [4] the main peak period of 5 s was selected. If accurate data become available the wave cover statistics can be re-evaluated.

### 2.4 Sea Surface Simulation

Once a wave spectrum is available a realistically-looking model of the sea surface can be reconstructed using the inverse transformation procedure similar to the one proposed by Massel [8]; this procedure is described in Appendix A. While the reconstructed sea surface is not the same as the initial real one, it looks realistic enough for our purpose, see Figure 5.

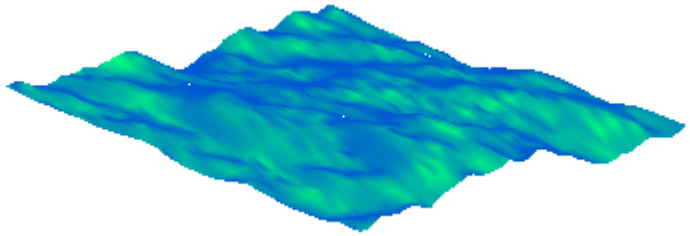

*Figure 5. A simulated sea surface with significant wave height 1.25 m, peak period 5 s. To make picture representative an area of 32 by 32 m was chosen.*

# 3. Target Cover by Waves as a Geometrical Problem

Once the sea surface elevation is known, the instant target visibility can be estimated. The target and the observer (or the gun) are placed on the reconstructed sea surface and connected by the line of sight. The sea surface immediately below the line of sight can be reconstructed by cutting through the sea surface with a vertical plane containing the line of sight, as shown on Figure 6 for a particular moment of time.

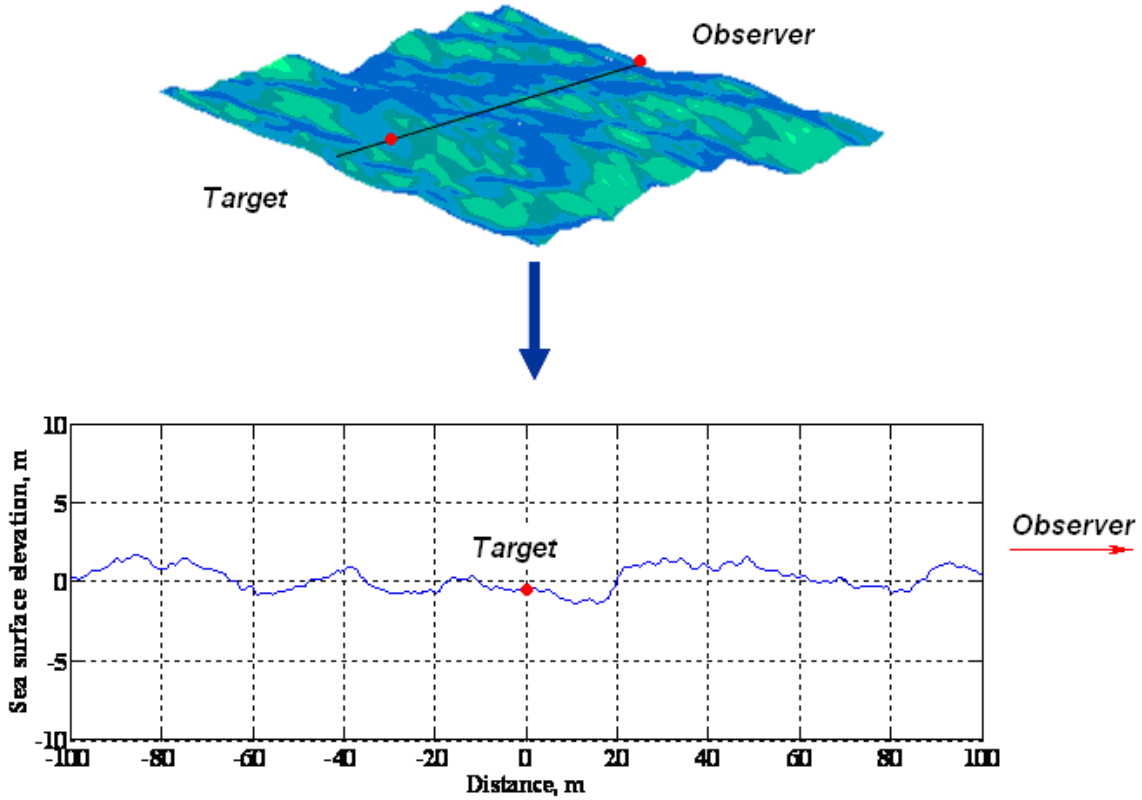


*Figure 6. An example how the sea surface elevation is seen in the vertical plane connecting the target and the observer*

Once the sea surface footprint on this vertical plane is known, the target visibility problem is reduced to a geometrical problem similar to a high-school "height of the tree shade" problem, see Figure 7. It is a simple problem if the tree location is known, but in the case of wave cover it is not known which particular wave crest is "casting shade", or providing cover to the target. For this reason the geometrical procedure is more involved than a textbook problem.

The problem is considered in a two-dimensional coordinate system where the horizontal $X$ axis connects the target and the observer's ship and $Z$ is the vertical axis, Figure 8. Zero level corresponds to calm sea level and origin of the $X$ axis is in the target position. Line AB represents the limiting line of sight: everything above this line is visible to the observer, and everything below it is invisible. Line AB touches the sea surface at least in one point, say C; at this stage its exact position is unknown. Point A' at the sea surface is the target waterline. An auxiliary line A'B' with origin in the point A', which is parallel to line AB, is introduced to find height of the covered part of the target AA'. Two situations are possible.

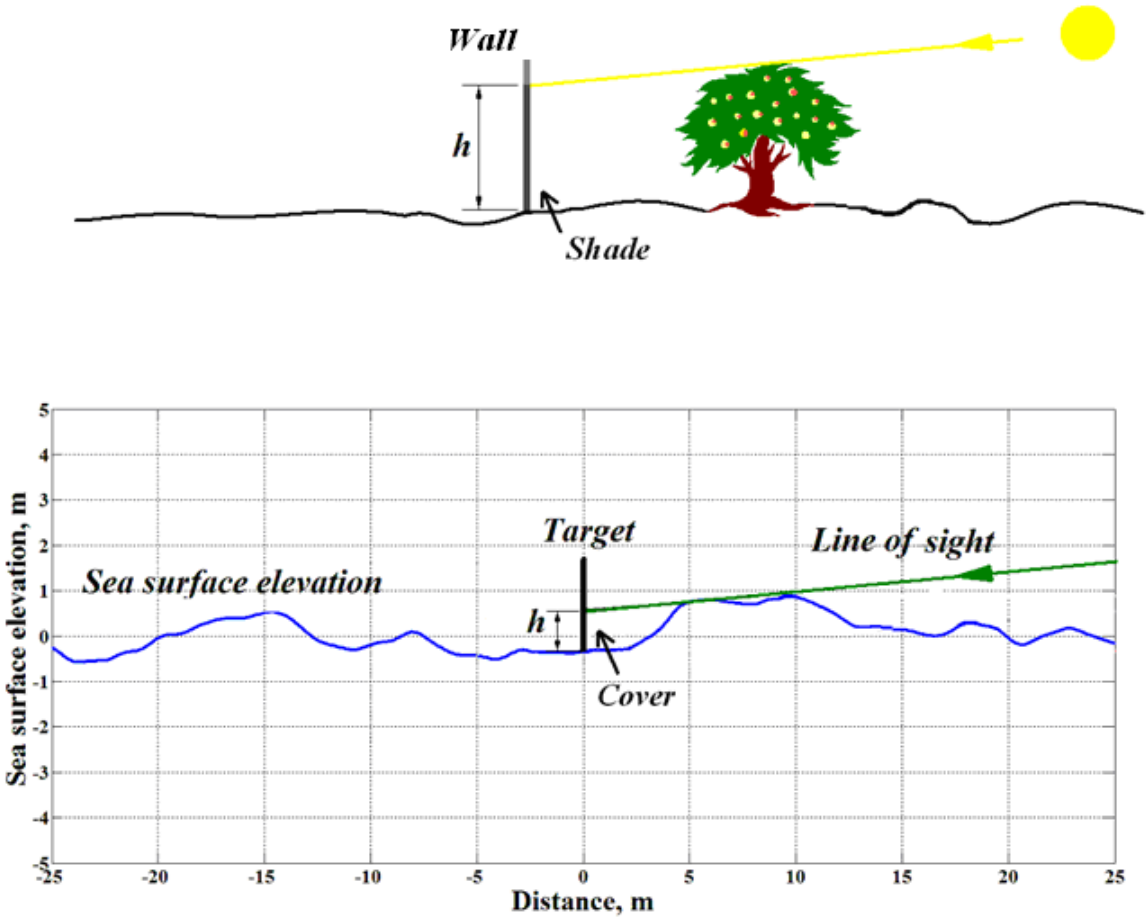


*Figure 7. Wave cover as a geometrical problem*

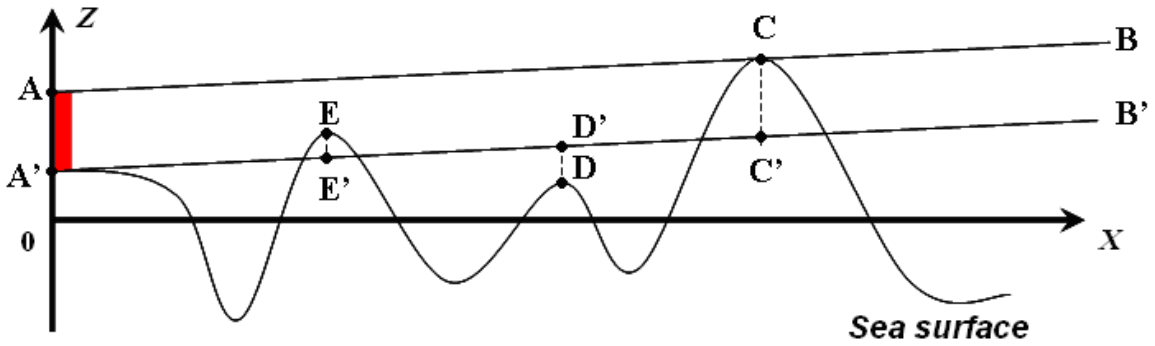


*Figure 8. Schematic diagram to the geometrical problem*

If the line A'B' goes above the sea surface, as illustrated by points D' and D on Figure 9 a, the difference between vertical coordinates of the line and the sea surface in point D is positive. Hence, if the "D" wave crest was the highest one between the observer and the target, the target would be fully exposed to the observer.

If some segments of the line A'B' go below the sea surface, as illustrated at points E' and C' on Figure 9 b, the differences between vertical coordinates of the line and the sea surface at the points E and C are negative. The segment EE' length is less than the segment CC' length; therefore, the target cover is defined by the "C" wave crest. In this situation the minimum of the difference between vertical coordinates of A'B' and sea surface is attained at the limiting point C, and this minimum is negative: the cover height AA' is equal to the segment CC' length. If the target is completely exposed the cover value is zero.

Mathematically, our findings can be expressed as follows:

$$\text{target cover} = \begin{cases} 0, \text{if } \min\left(z'(x) - z(x)\right) \geq 0, \\ -\min\left(z'(x) - z(x)\right) \text{ otherwise,} \end{cases}$$

where $z'(x)$ and $z(x)$ are vertical coordinates of points on the A'B' line and the sea surface, respectively.

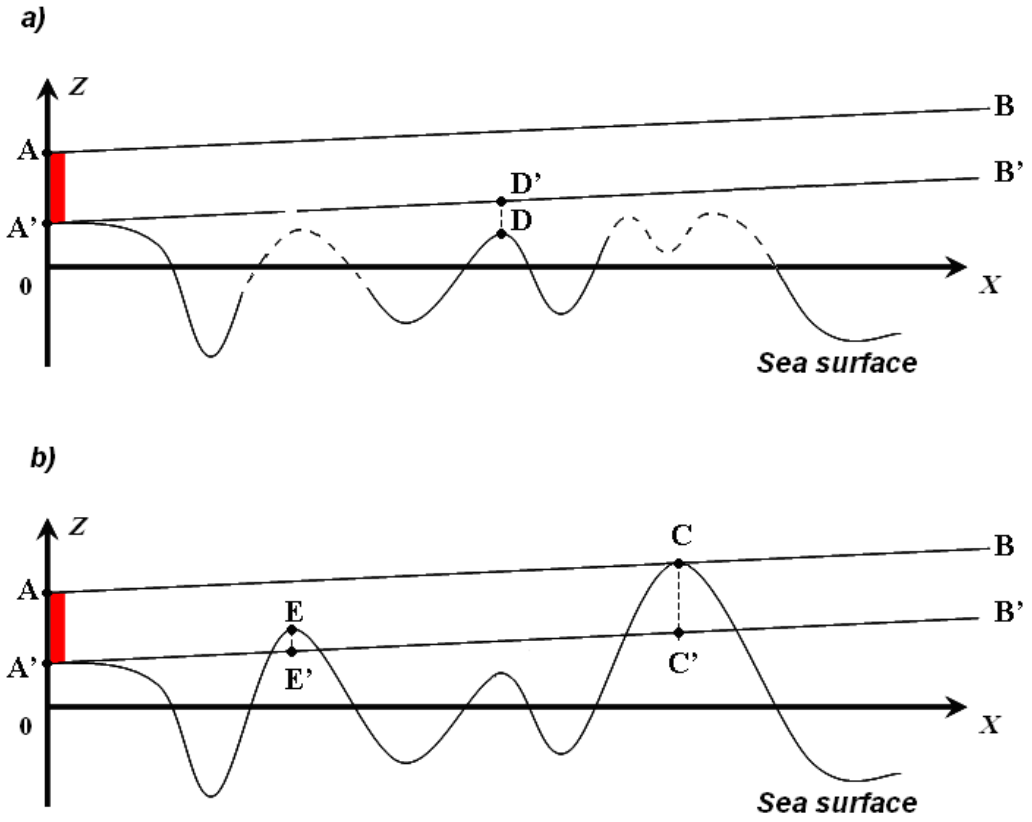


*Figure 9. Two possible situations: a) the target is not covered and b) the target is covered*

Since the sea surface moves, the algorithm for calculating the target cover finds the cover value at each predefined moment of time over a chosen time interval and produces a time series of the wave cover values.

The target cover depends on the angle of sight, significant wave height, wave direction, and speed of the target. The target cover should decrease with increase in angle of sight, as it is illustrated on Figure 10. The target cover should increase with increase in wave height, as shown on Figure 11. Effect of wave direction and target speed on target visibility are not governed by geometry of the sea surface alone; these effects will be considered on particular examples in the next section.

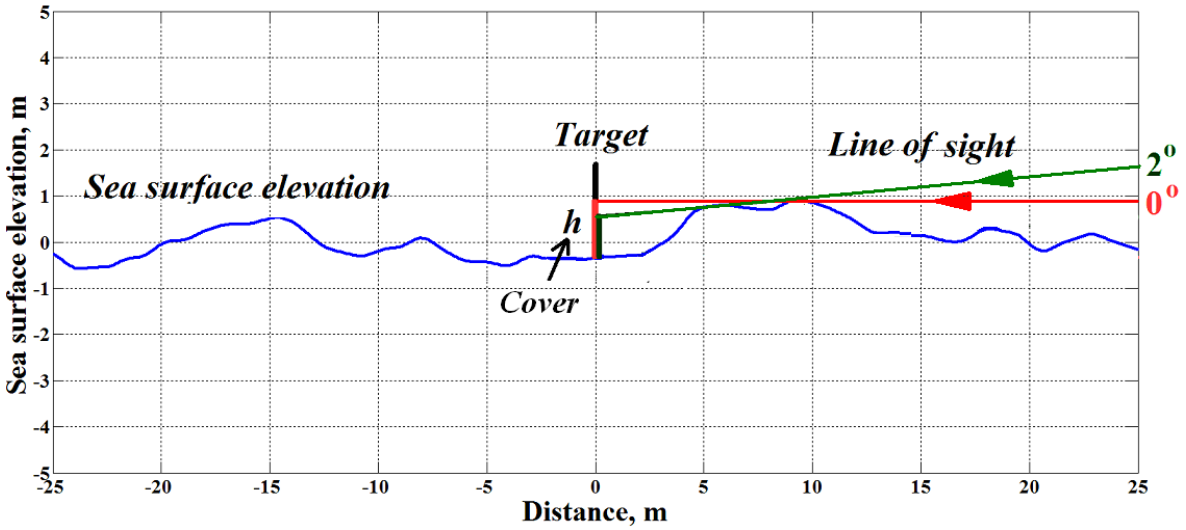


*Figure 10. Expected effect of different angle of sight on target cover*

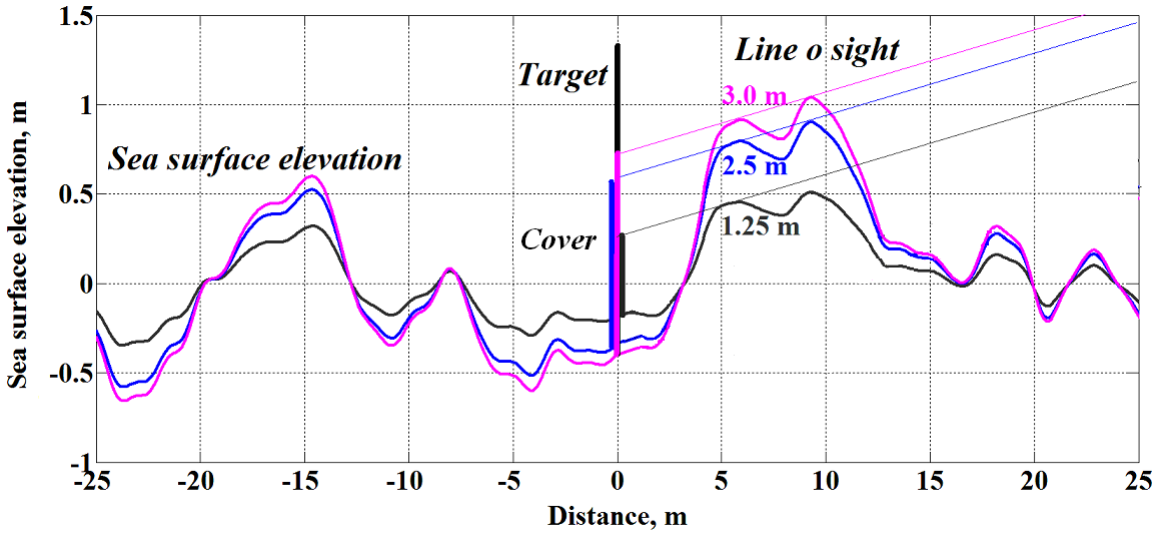


*Figure 11. Expected effect of significant wave height on target cover*

# 4. Results of simulation

## 4.1 Time Series

The target visibility simulations were carried out with input parameters listed in Table 2, resulting in total 1125 simulated target cover time series of 257 data points each. The resultant multidimensional data array occupies approximately 2.3 megabytes of computer memory. Examples of the simulated time series (truncated at 30 s) are shown on Figure 13 and Figure 14.

The model behaved as expected with change of input parameters: increase of angle of sight caused decrease of wave cover; increase of the significant wave height resulted in higher and longer cover.

*Table 2. Input parameters for simulation*

| Parameter | Values or range |
|---|---|
| Angle of sight (angle of fall)<br>Wave direction<br>Significant wave height<br>Target speed<br>Time | $0^o$…$25^o$, $1^o$ step<br>$0^o$…$180^o$ degrees, $45^o$ step, see Figure 12<br>1.25 m, 2.5 m, 3.0 m<br>0, 20, 40 knots<br>0…64 s, 0.25 s step |

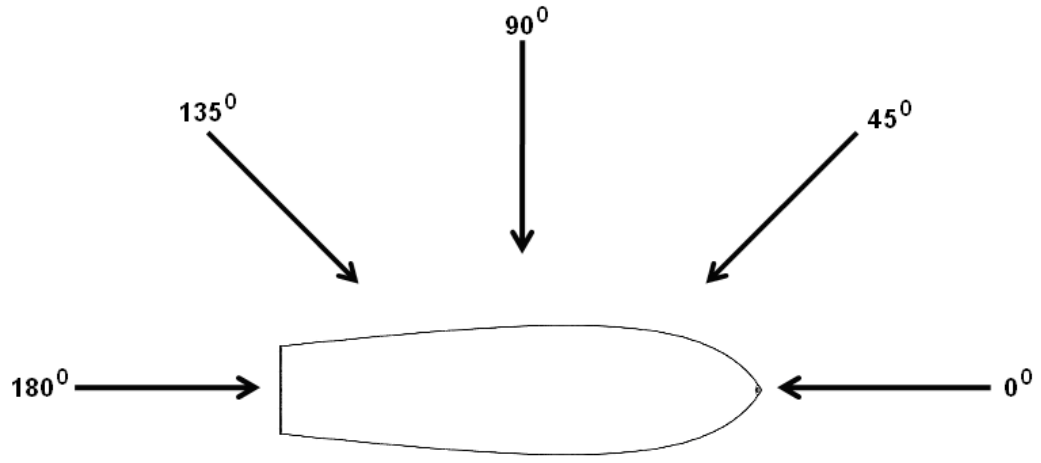


*Figure 12. Wave direction in relation to the target*

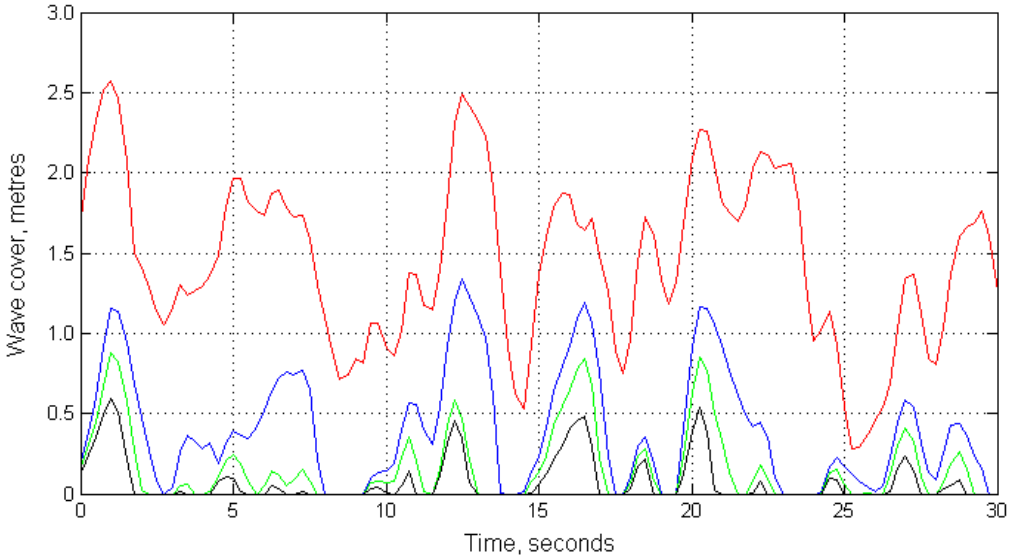


*Figure 13. Wave cover vs time. Angle of sight: red, 0º; blue, 2º; green, 4º; and black, 6º. Wind direction, significant wave height, and target speed remained the same.*

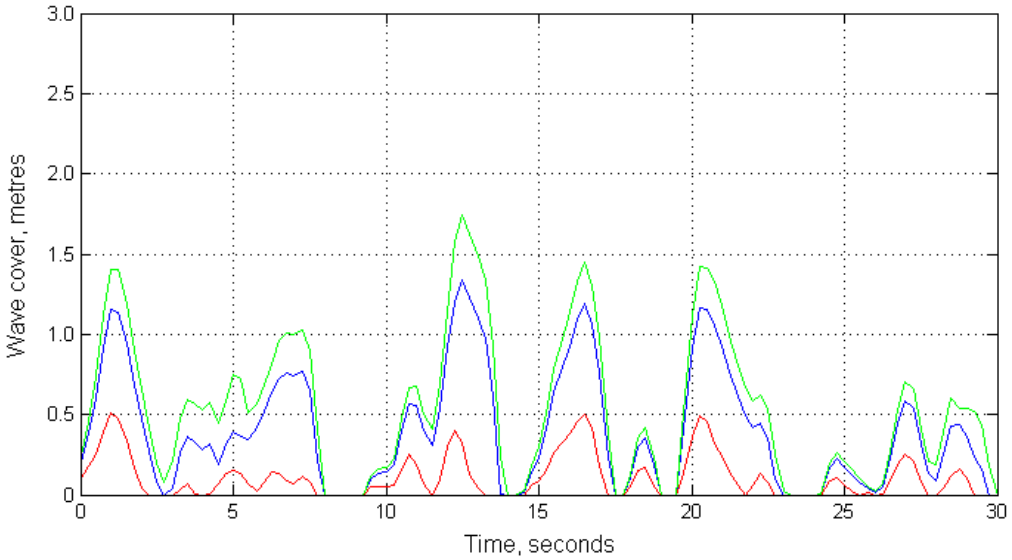


*Figure 14. Wave cover for different significant wave heights: red, 1.25 m; blue, 2.5 m; green, 3 m. Wind direction, angle of sight, and target speed remained the same.*

## 4.2 Using Wave Cover Data in Weapons Performance Analysis

The time the wave cover model takes to build the sea surface and sheer amount of data produced makes it problematic to feed the raw wave cover data into a weapons performance model even for a single run; the raw data feeding becomes nearly impossible if the weapons performance model takes a few hundreds Monte-Carlo runs. A simplified approach to gun performance analysis is suggested to overcome this difficulty. The essence of this method is using the wave cover data to calculate expected overall decrease in ammunition effectiveness first rather than feeding the wave cover data straight into the gun fire model on the round-by-round basis.

For armour-piercing and high-explosive rounds the wave cover effect can be modelled by reducing ammunition effectiveness, keeping the probability of hit unchanged:

$$P'_{k|h} = \mu P_{k|h},$$

where $P_{k|h}$ is the probability of a component kill or personnel incapacitation given a hit, $P'_{k|h}$ stands for the reduced probability of kill of incapacitation given a hit, and $\mu$ is the ammunition effectiveness coefficient. If the target is completely hidden behind waves, the ammunition effectiveness coefficient is 0; if the target is completely exposed, the coefficient is 1.

Air-burst munitions require different treatment, as they usually deliver multiple hits on the target and the ammunition effectiveness depends on the stand-off distance. However even in this case wave cover effect can be modelled by reducing round effectiveness, keeping other parameters unchanged.

The mathematical background of this approach is presented in Appendix B:

The raw wave cover data was processed following this approach such that a weapon performance model could use the wave cover statistics instead.

## 4.3 Frequency Distributions

First, all wave cover data was processed using the moving average method filtering out the high-frequency "jiggle" of the data. The data was processed with 0.5 s, 1.0s, and 5.0 s averaging windows. Next, the averaged data were sorted in bins of 0.1 m; the other input parameters remained as are listed in Table 2. The process produced 3510 histograms in total ($3 \times 3 \times 26 \times 5 \times 3$). It was still deemed too many, so the following steps were taken to further reduce the data amount:

1. At angles of impact at and above 8° there is virtually no significant cover, see for example Figure 15; hence the number of angles of impact was limited to five values: 0, 2, 4, 6 and 8 degrees, with interpolation for interim angles and assumption of no cover for angles above 8°.

2. Data for 5 s window was excluded after a discussion as so lengthy continuous engagement is unlikely in practice. The wave cover frequency distribution for 0.5 s and 1 s sliding windows were really close, as exemplified on Figure 16. Therefore, data for 1 s window size could be used in the weapons performance analysis.

3. The frequency distributions were rather close for various target speed and wave direction, as illustrated on Figure 17 and Figure 18; it was also assumed that in reality the target speed and orientation would be random. Hence the remaining data was averaged by target speed and wave direction.

Finally, wave cover frequency distributions were obtained for:

- averaging window size of 1 s (1 value),
- wave height of 1.25 m, 2.5 m, and 3.0 m (3 values),
- angles of sight/impact of 0°, 2°, 4°, 6°, and 8° (5 values).

In total this process resulted in $1 \times 3 \times 5 = 15$ frequency distributions. Some of the distributions are shown on Figure 19; the tabulated data is listed in Appendix C:

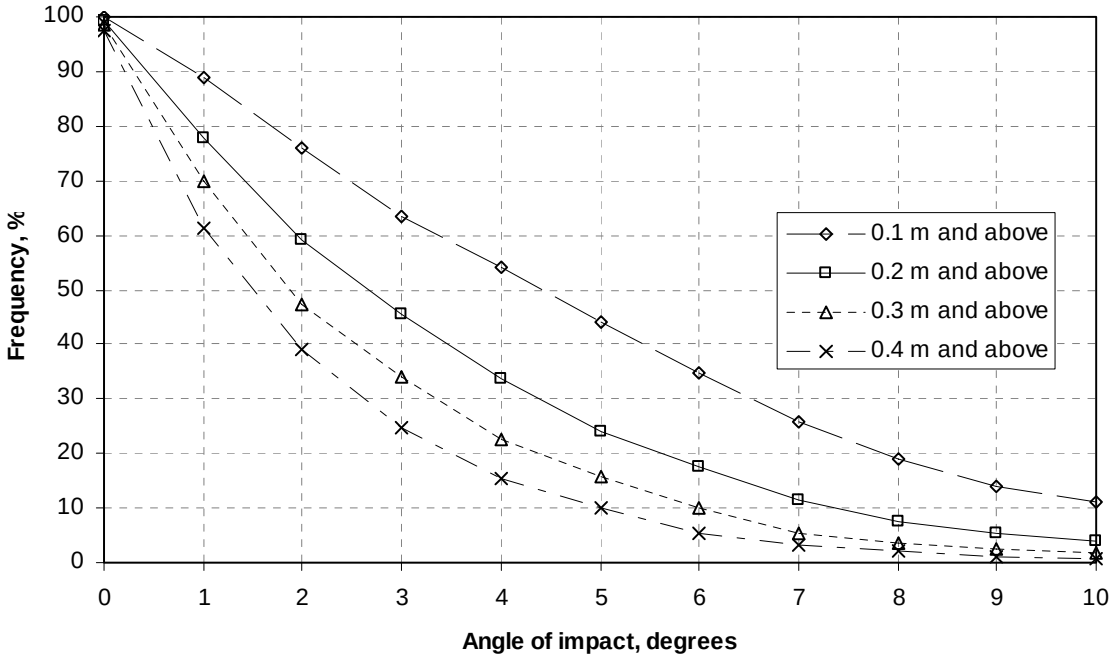


*Figure 15. Frequency of wave cover above certain height depending on the angle of impact; averaging window 1 s, wave height 2.5 m, target speed 0 knots, wave direction 0°.*

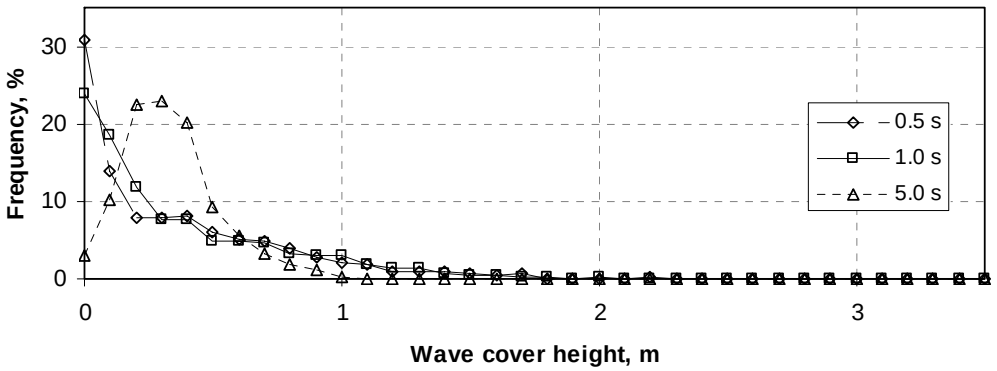


*Figure 16. Wave cover frequency distribution for 0.5s, 1.0s, and 5.0 s averaging window; all other simulation parameters remained the same: wave height 2.5 m, target speed 0 knots, wave direction 0°, angle of impact 2°.*

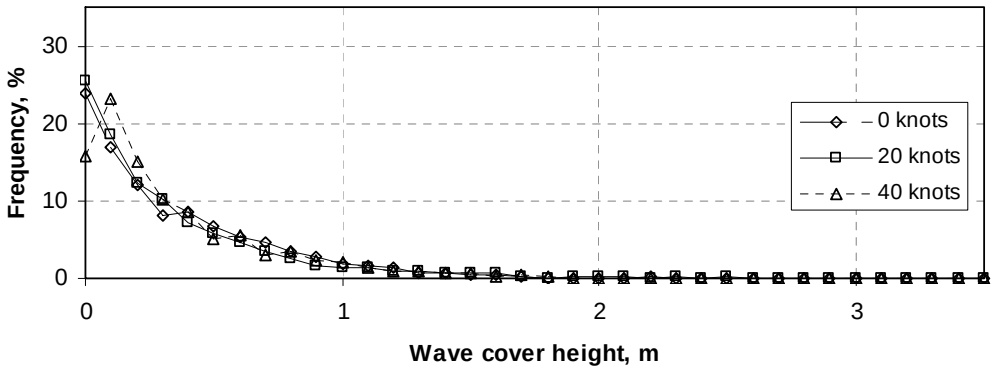


*Figure 17. Wave cover frequency distribution for 0 knots, 20 knots, and 40 knots target speed; all other simulation parameters remained the same: wave height 2.5 m, averaging window 1 s, wave direction 0°, angle of impact 2°.*

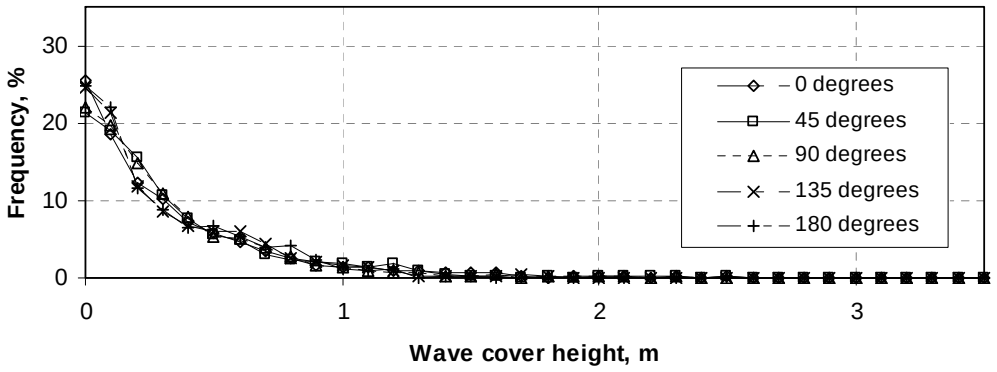


*Figure 18. Wave cover frequency distribution for five different wave directions; all other simulation parameters remained the same: wave height 2.5 m, averaging window 1 s, target speed 20 knots, angle of impact 2°.*

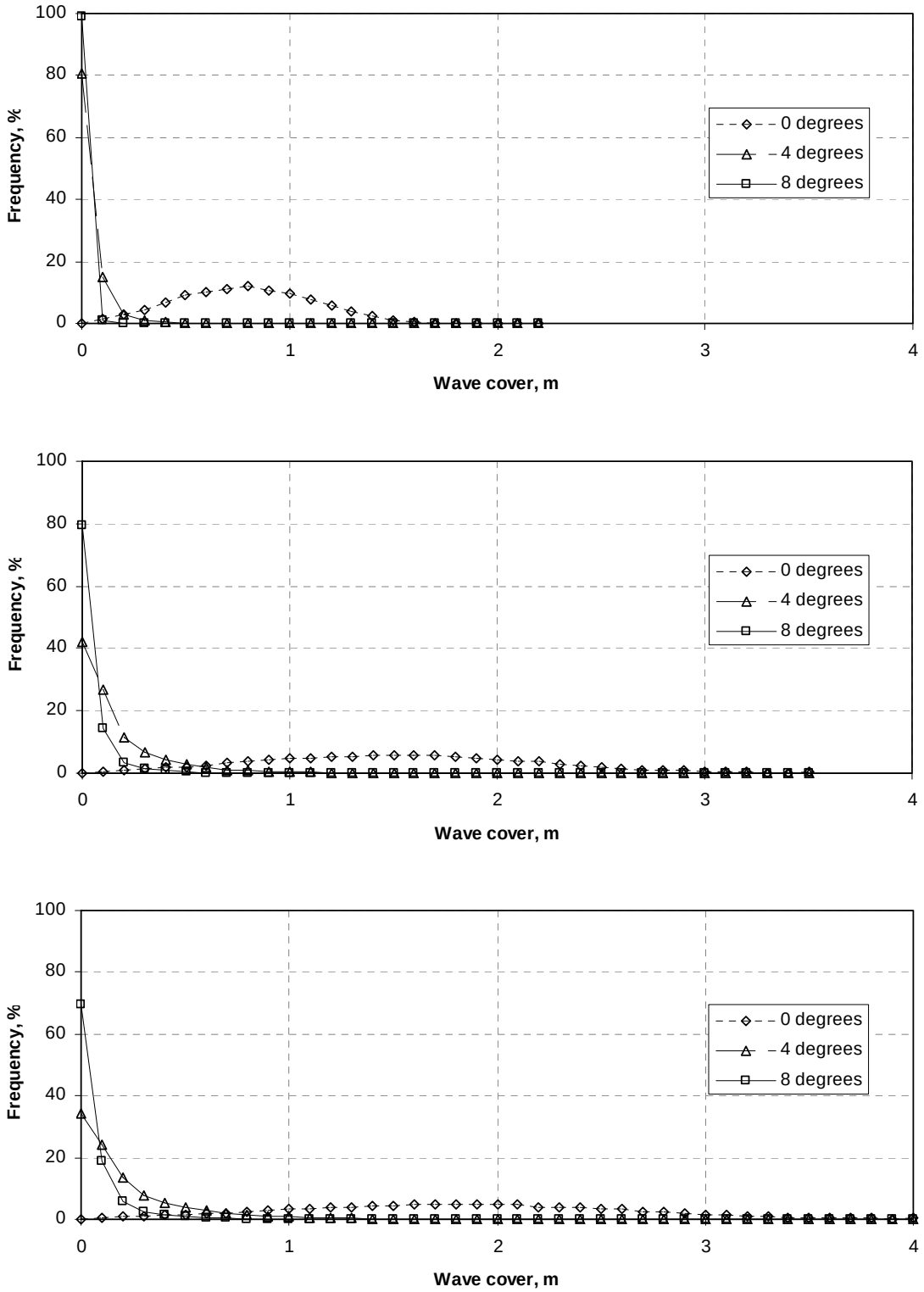


*Figure 19. Wave cover frequency distribution for significant wave height of 1.25 m (top), 2.5 m (centre), and 3.0 m (bottom); different curves correspond to different angles of impact, as shown on the legends.*

# 5. Conclusion

## 5.1 Summary

The initial wave cover problem stated in the Introduction was analysed and investigations were conducted in the following directions:

1. Analysing randomly moving sea surface models and suggesting a suitable model for the requires condition;
2. Analysing geometry of target cover by waves;
3. Performing statistical analysis of the wave cover; and
4. Looking at practical use of the simulated data for a naval gun / ammunition performance analysis.

Real oceanographic data for the area of interest could not be obtained in time for this project; therefore, the Soares-Torsethaugen spectral model was used as a closest available approximation to oceanographic situation in the area of interest since it describes combined action of wind and swell with limited fetch in coastal water. Note that due to insufficient time no sensitivity study was conducted.

Finding the target cover height was considered as a two-dimensional geometrical problem; no consideration was given to change of actual cover along the target waterline or for the target pitch and roll (e.g. the bow is completely covered by waves and the stem is completely exposed). A mathematical expression for the cover height for this simplified geometrical model was derived.

The computer model of wave cover behaved as expected: increase of angle of sight caused decrease of wave cover, increase of wave height resulted in higher and longer cover. Target speed and wave direction did not affect significantly the cover height. A single simulation run resulted in 1125 time series of 257 values each, making it difficult to use the wave cover model in Monte-Carlo-based weapon performance evaluation. Statistical processing of the raw wave cover simulation data made it possible to reduce the data amount significantly, and the final wave cover data were presented as 15 frequency distributions for wave heights of 1.25, 2.5 and 3 m and angles of sight of 0, 2, 4, 6, and 8 degrees.

It was suggested to model the effect of wave cover on gun performance by introducing the ammunition effectiveness coefficient derived from the wave cover height. The ammunition effectiveness coefficient for armour-piercing and point detonation high explosive rounds is equal to the ratio of exposed target area and the total target area. The air burst munitions require different treatment; the coefficient should be estimated depending on the individual fragment lethality, fragment density, and target cover by waves.

### 5.2 Future Work

It is suggested to aim the future work in modelling of floating target behaviour in rough seas on improving the weapon firing modelling and developing a fast but realistic method of sea cover modelling. A future weapon firing model should be able to change target vulnerable area and/or round lethality on the round-to-round base. Combined with ability to simulate a realistic wave cover as a time series would enhance the future weapon performance analysis capability.

## 6. Acknowledgement

The author would like to thank LCDR Kim Baddams for help with oceanographic data for this project.

# References

1. Fedosov A.N, Filimonov I.L. *Modelling of Sea Surface Waves for Applied Problems*. Collection of Scientific Works of Nakhimov Navy Academy, Sevastopol, Ukraine, issue 3, 2010, pp. 45-55 (in Russian)
2. Guedes Soares, C. *Representation of double-peaked sea wave spectra*. Ocean Engineering, vol. 11, issue 2, 1984, pp. 185-207.
3. Hasselmann, K., T.P. Barnett, E. Bouws, H. Carlson, D.E. Cartwright, K. Enke, J.A. Ewing, H. Gienapp, D.E. Hasselmann, P. Kruseman, A. Meerburg, P. Müller, D.J. Olbers, K. Richter, W. Sell and H. Walden. *Measurements of wind-wave growth and swell decay during the Joint North Sea Wave Project (JONSWAP)*. Erganzungsheft zur Deutsche Hydrographische Zeitschrift, Reihe A($8^0$) Nr. 12, 1973, pp 1-95.
4. Hogben, N., Dacunha, N. M. C., Olliver, G. F. *Global Wave Statistics*. Published for British Maritime Technology by Unwin Brothers, London, UK, 1986.
5. *Kon-Tiki photo gallery*. Answers Corporation, St. Louis, USA. Viewed 3 December 2012, < http://www.answers.com/topic/kon-tiki-large-image>.
6. Longuet-Higgins, M. S. *Statistical Properties of an Isotropic Random Surface.* Philosophical Transactions of the Royal Society in London, Ser. A: Mathematical and Physical Sciences, vol. 250, № 975, 1957, pp. 157-174.
7. *Marine Weather Definitions*. Bureau of Meteorology, Canberra. Viewed 3 December 2012, <http://www.bom.gov.au/marine/about/marine-definitions.shtml>.
8. Massel, S.R. *Ocean Surface Waves: Their Physics and Prediction*. World Scientific, Singapore, 1996.
9. Ochi, M. K., Hubble, E. N. *On six-parameter wave spectra*. Proceedings of the 15th Conference on Coastal Engineering, Honolulu, Hawaii, 1976, pp. 301-329.
10. Pierson, W. J., and Moskowitz, L. *A proposed spectral form for fully developed wind seas based on the similarity theory of S. A. Kitaigorodskii*. Journal of Geophysical Research, vol. 69, issue 24, 1964, pp 5181-5190.
11. *The Specialist Committee on Environmental Modeling Final Report and Recommendations to the 22nd ITTC*. Proceedings of the 22nd International Towing Tank Conference, Seoul and Shanghai, 1999. Viewed 3 December 2012, <http://ittc.sname.org/contents.htm>.
12. *The Specialist Committee on Waves Final Report and Recommendations to the 23rd ITTC*. Proceedings of the 23rd International Towing Tank Conference, Venice, Italy, 2002, vol. II, pp. 505-551.
13. Torsethaugen, K. *A two peak wave spectrum model.* Proceeding of the 12th International Conference on Offshore Mechanics and Arctic Engineering, Glasgow, UK, 1993, vol. II, pp. 175-181.
14. Torsethaugen, K. *Simplified double peak spectral model for ocean waves*. SINTEF Report STF80 A048052, SINTEF Fisheries and Aquaculture, Trondheim, Norway, 2004.

*This page is intentionally blank*

# Appendix A: Wave Spectra and Simulation Technique

## A.1 Wave Spectrum

The Wiener-Khinchine theorem states that the autocorrelation function of a stationary random process has a spectral decomposition given by the power spectrum of that process.

To put the theorem into the oceanographic context, it is assumed that the sea surface can be represented as a sum of harmonic waves:

$$\zeta(x,y,t)=\sum_{n=1}^{N} a_n \cos(-k_{xn}x-k_{yn}y+\omega_n t+\varepsilon_n), \tag{A.1}$$

where:
$x$ and $y$ – coordinates of the point on the sea surface;
$t$ – time;
$a_n$ – wave amplitude;
$k_{xn}$ and $k_{yn}$ – are projections of two-dimensional wave vector on X and Y axis respectively;
$\omega$ – wave frequency;
$\varepsilon$- random wave phases uniformly distributed in the interval (0, 2π);
$N$ is the number of harmonic waves taken into account;
subscript $n$ means all parameters are specific for the $n^{th}$ harmonic wave.

The autocorrelation function describes sea surface without using random parameters:

$$\psi(\xi,\eta,\tau)=\lim_{X,Y,T\to\infty}\frac{1}{8XYT}\int_{-X}^{X}\int_{-Y}^{Y}\int_{-T}^{T}\zeta(x,y,t)\zeta(x+\xi,y+\eta,t+\tau)dxdydt, \tag{A.2}$$

The autocorrelation function for irregular waves quickly vanishes as absolute values of $\xi$, $\eta$, and $\tau$ increase, but for regular waves the function remains non-zero at relatively large absolute values of $\xi$, $\eta$, and $\tau$.

The following trigonometric identities are used in the further calculations:

$$\cos\alpha\cos\beta=\frac{1}{2}\left(\cos(\alpha-\beta)+\cos(\alpha+\beta)\right), \tag{A.3}$$

$$\sin\alpha-\sin\beta=2\left(\sin\left(\frac{\alpha-\beta}{2}\right)\cos\left(\frac{\alpha+\beta}{2}\right)\right). \tag{A.4}$$

Combining equations (A.1) and (A.3) yields the following expression:

$$\zeta(x,y,t)\zeta(x+\xi,y+\eta,t+\tau)=F_1(\xi,\eta,\tau)+F_2(x,y,t,\xi,\eta,\tau)+F_3(x,y,t,\xi,\eta,\tau)+F_4(x,y,t,\xi,\eta,\tau), \tag{A.5}$$

where

$$F_1(\xi,\eta,\tau)=\sum_{i=1}^{N}\frac{a_i^2}{2}\cos\left(k_{xi}\xi+k_{yi}\eta-\omega_i\tau\right), \tag{A.6}$$

$$F_2(x,y,t,\xi,\eta,\tau)=\sum_{i=1}^{N}\frac{a_i^2}{2}\cos\left(-2k_{xi}x-2k_{yi}y+2\omega_i t-k_{xi}\xi-k_{yi}\eta+\omega_i\tau+2\varepsilon_i\right), \tag{A.7}$$

$$F_3(x,y,t,\xi,\eta,\tau)=$$
$$\sum_{i=1}^{N}\sum_{j\neq i}^{N}\frac{a_i a_j}{2}\cos\left(-\left(k_{xi}-k_{xj}\right)x-\left(k_{yi}-k_{yj}\right)y+\left(\omega_i-\omega_j\right)t+k_{xj}\xi+k_{yj}\eta-\omega_j\tau+\left(\varepsilon_i-\varepsilon_j\right)\right), \tag{A.8}$$

$$F_4(x,y,t,\xi,\eta,\tau)=$$
$$\sum_{i=1}^{N}\sum_{j\neq i}^{N}\frac{a_i a_j}{2}\cos\left(-\left(k_{xi}+k_{xj}\right)x-\left(k_{yi}+k_{yj}\right)y+\left(\omega_i+\omega_j\right)t-k_{xj}\xi-k_{yj}\eta+\omega_j\tau+\left(\varepsilon_i+\varepsilon_j\right)\right). \tag{A.9}$$

Equations (A.6)–(A.9) are substituted into equation (A.5), the result is substituted into equation (A.2), and then each member is calculated separately, as follows:

$$\int_{-X}^{X}\int_{-Y}^{Y}\int_{-T}^{T}F_1(\xi,\eta,\tau)\,dxdydt=$$
$$\sum_{i=1}^{N}\frac{a_i^2}{2}\cos\left(k_{xi}\xi+k_{yi}\eta-\omega_i\tau_i\right)\int_{-X}^{X}\int_{-Y}^{Y}\int_{-T}^{T}dxdydt=$$
$$8XYT\sum_{i=1}^{N}\frac{a_i^2}{2}\cos\left(k_{xi}\xi+k_{yi}\eta-\omega_i\tau_i\right), \tag{A.10}$$

$$\lim_{X,Y,T\to\infty}\frac{1}{8XYT}\left(8XYT\sum_{i=1}^{N}\frac{a_i^2}{2}\cos\left(k_{xi}\xi+k_{yi}\eta-\omega_i\tau_i\right)\right)=\sum_{i=1}^{N}\frac{a_i^2}{2}\cos\left(k_{xi}\xi+k_{yi}\eta-\omega_i\tau_i\right). \tag{A.11}$$

For $F_2$, let $\gamma_i = -k_{xi}\,\xi - k_{yi}\,\eta + \omega_i\,\tau + 2\,\varepsilon_i$ be the part of the cosine argument which does not depend on $x$, $y$, $t$; then:

$$\int_{-X}^{X}\int_{-Y}^{Y}\int_{-T}^{T} F_2(x,y,t,\xi,\eta,\tau)\,dxdydt =$$

$$\int_{-X}^{X}\int_{-Y}^{Y}\int_{-T}^{T}\sum_{i=1}^{N}\frac{a_i^2}{2}\cos\left(-2k_{xi}x-2k_{yi}y+2\omega_i t+\gamma_i\right)dxdydt =$$

$$\int_{-Y}^{Y}\int_{-T}^{T}\sum_{i=1}^{N}\left(-\frac{a_i^2}{2k_{xi}}\right)\left(\sin\left(-2k_{xi}x-2k_{yi}y+2\omega_i t_i+\gamma_i\right)\Big|_{-X}^{X}\right)dydt =$$

$$\int_{-Y}^{Y}\int_{-T}^{T}\sum_{i=1}^{N}\frac{a_i^2}{2}\frac{\sin(2k_{xi}X)}{k_{xi}}\cos\left(-2k_{yi}y+2\omega_i t+\gamma_i\right)dydt =$$

$$\int_{-T}^{T}\sum_{i=1}^{N}\frac{a_i^2}{2}\frac{\sin(2k_{xi}X)}{k_{xi}}\frac{\sin(2k_{yi}Y)}{k_{yi}}\cos(2\omega_i t+\gamma_i)ydt =$$

$$\sum_{i=1}^{N}\left(-\frac{a_i^2}{2}\right)\frac{\sin(2k_{xi}X)}{k_{xi}}\frac{\sin(2k_{yi}Y)}{k_{yi}}\frac{\sin(2\omega_i T)}{\omega_i}\cos\gamma_i, \qquad \text{(A.12)}$$

$$\lim_{X,Y,T\to\infty}\frac{1}{8XYT}\sum_{i=1}^{N}\left(-\frac{a_i^2}{2}\right)\frac{\sin(2k_{xi}X)}{k_{xi}}\frac{\sin(2k_{yi}Y)}{k_{yi}}\frac{\sin(2\omega_i T)}{\omega_i}\cos\gamma_i = 0. \qquad \text{(A.13)}$$

A new notation is introduced to simplify transformation of expressions for $F_3$ and $F_4$, namely:

$$k_{xij-} = k_{xi} - k_{xj},\quad k_{yij-} = k_{yi} - k_{yj},\quad \omega_{ij-} = \omega_i - \omega_j,\quad \gamma_{ij-} = k_{xj}\xi + k_{yj}\eta - \omega_j\tau + (\varepsilon_i - \varepsilon_j),$$
$$k_{xij+} = k_{xi} + k_{xj},\quad k_{yij+} = k_{yi} + k_{yj},\quad \omega_{ij+} = \omega_i + \omega_j,\quad \gamma_{ij+} = -k_{xj}\xi - k_{yj}\eta + \omega_j\tau + (\varepsilon_i + \varepsilon_j).$$

Then :

$$\int_{-X}^{X}\int_{-Y}^{Y}\int_{-T}^{T} F_3(x,y,t,\xi,\eta,\tau)\,dxdydt =$$

$$\int_{-X}^{X}\int_{-Y}^{Y}\int_{-T}^{T}\sum_{i=1}^{N}\sum_{j\neq i}^{N}\frac{a_i a_j}{2}\cos\left(-k_{xij-}x-k_{yij-}y+\omega_{ij-}t+\gamma_{ij-}\right)dxdydt =$$

$$\int_{-Y}^{Y}\int_{-T}^{T}\sum_{i=1}^{N}\sum_{j\neq i}^{N}\left(-\frac{a_i a_j}{2k_{xij-}}\right)\left(\sin\left(-k_{xij-}x-k_{yij-}y+\omega_{ij-}t_i+\gamma_{ij-}\right)\Big|_{-X}^{X}\right)dydt =$$

$$\int_{-Y}^{Y}\int_{-T}^{T}\sum_{i=1}^{N}\sum_{j\neq i}^{N}\frac{a_i a_j}{4}\frac{\sin(k_{xij-}X)}{k_{xij-}}\cos\left(-k_{yij-}y+\omega_{ij-}t+\gamma_{ij-}\right)dydt =$$

$$\int_{-T}^{T}\sum_{i=1}^{N}\sum_{j\neq i}^{N}\frac{a_i a_j}{8}\frac{\sin(k_{xij-}X)}{k_{xij-}}\frac{\sin(k_{yij-}Y)}{k_{yij-}}\cos(2\omega_{ij-}t+\gamma_{ij-})ydt =$$

$$\sum_{i=1}^{N}\sum_{j\neq i}^{N}\left(-\frac{a_i a_j}{16}\right)\frac{\sin(2k_{xij-}X)}{k_{xij-}}\frac{\sin(2k_{yij-}Y)}{k_{yij-}}\frac{\sin(2\omega_{ij-}T)}{\omega_{ij-}}\cos\gamma_{ij-}, \qquad \text{(A.14)}$$

$$\lim_{X,Y,T\to\infty}\frac{1}{8XYT}\sum_{i=1}^{N}\sum_{j\neq i}^{N}\left(-\frac{a_i a_j}{16}\right)\frac{\sin\left(k_{xij-}X\right)}{k_{xij-}}\frac{\sin\left(k_{yij-}Y\right)}{k_{yij-}}\frac{\sin\left(\omega_{ij-}T\right)}{\omega_{ij-}}\cos\gamma_{ij-}=0. \tag{A.15}$$

Similarly,

$$\int_{-X}^{X}\int_{-Y}^{Y}\int_{-T}^{T}F_4(x,y,t,\xi,\eta,\tau)dxdydt = \sum_{i=1}^{N}\sum_{j\neq i}^{N}\left(-\frac{a_i a_j}{16}\right)\frac{\sin\left(2k_{xij+}X\right)}{k_{xij+}}\frac{\sin\left(2k_{yij+}Y\right)}{k_{yij+}}\frac{\sin\left(2\omega_{ij+}T\right)}{\omega_{ij+}}\cos\gamma_{ij+}, \tag{A.16}$$

$$\lim_{X,Y,T\to\infty}\frac{1}{8XYT}\sum_{i=1}^{N}\sum_{j\neq i}^{N}\left(-\frac{a_i a_j}{16}\right)\frac{\sin\left(k_{xij+}X\right)}{k_{xij+}}\frac{\sin\left(k_{yij+}Y\right)}{k_{yij+}}\frac{\sin\left(\omega_{ij+}T\right)}{\omega_{ij+}}\cos\gamma_{ij=}=0. \tag{A.17}$$

Taking equations (A.11), (A.13), (A.15), and (A.17) into account, it can be concluded that:

$$\psi(\xi,\eta,\tau)=\sum_{i=1}^{N}\frac{a_i^2}{2}\cos\left(k_{xi}\xi+k_{yi}\eta-\omega_i\tau_i\right). \tag{A.18}$$

The Fourier transform (the cosine transform as real values only are considered) of the autocorrelation function is then taken to obtain the wave spectrum in accordance with the Wiener-Khinchine theorem, as follows:

$$\begin{aligned}E_j &= \lim_{X,Y,T\to\infty}\frac{1}{8XYT}\int_{-X}^{X}\int_{-Y}^{Y}\int_{-T}^{T}\psi(\xi,\eta,\tau)\cos(k_{xj}\xi+k_{yj}\eta-\omega_j\tau)d\xi d\eta d\tau\\ &= \lim_{X,Y,T\to\infty}\frac{1}{8XYT}\int_{-X}^{X}\int_{-Y}^{Y}\int_{-T}^{T}\sum_{i=1}^{N}\frac{a_i^2}{2}\cos(k_{xi}\xi+k_{yi}\eta-\omega_i\tau)\cos(k_{xj}\xi+k_{yj}\eta-\omega_j\tau)d\xi d\eta d\tau\\ &= \frac{a_j^2}{2}.\end{aligned} \tag{A.19}$$

Therefore, energy of the $j$-th harmonic wave is equal to $a_j^2/2$; $j = 1\ldots N$.

Let $\theta_i$ be the propagation direction of the $j$-th harmonic wave measured counterclockwise from the $x$-axis; then the wave vector components can be expressed as follows:

$$k_{xi}=k_i\cos\theta_i,\quad k_{yi}=k_i\sin\theta_i, \tag{A.20}$$

The wave vector magnitude $k_j$ and the wave frequency $\omega_j$ are related by the following deep-water dispersion relation:

$$\omega_j^2=gk_j, \tag{A.21}$$

where $g$ is the gravity acceleration. Since the harmonic waves were initially indexed in an arbitrary manner, it is more logical to describe each wave in terms of its energy, direction

and frequency, noting that each pair ($\omega_i$, $\theta_i$) is unique; therefore the power spectrum can be expressed as a function of two variables, ($\omega_i$, $\theta_i$), as follows:

$$E_j = E(\omega_j, \theta_j), \tag{A.22}$$

where $E(\omega, \theta)$ is the discrete directional wave spectrum.

A continuous wave spectrum $S(\omega, \theta)$ is obtained by a similar process with sums substituted by integrals; for example, equation (A.1) should be rewritten as follows:

$$\zeta(x, y, t) = \int_0^{\infty} \int_{-\pi}^{\pi} a(\omega, \theta) \cos(-kx \cos\theta - ky \sin\theta + \omega t + \varepsilon)\ d\theta\ d\omega .$$

Since only the finite sums are used in this simulation, the detailed derivation of the continuous spectrum is not presented here.

## A.2 Sea Surface Simulation

The sea surface evolution can be simulated from the known directional spectrum using equation (A.1) as a starting point:

$$\tilde{\zeta}(x, y, t) = \sum_{i=1}^{N} \tilde{a}_i \cos(-k_i x \cos\theta_i - k_i y \sin\theta_i + \omega_i t + \tilde{\varepsilon}_i), \tag{A.23}$$

where:
$\tilde{\zeta}$ is the simulated sea surface height,
$\tilde{a}_i$ is the $i$-th wave amplitude calculated from the energy spectrum,
$\tilde{\varepsilon}_i$ is the $i$-th wave random phase,
$\theta_i$ is the $i$-th harmonic wave propagation direction,
the wave vector of the $i$-th harmonic wave, $k_i$, is linked to the wave frequency $\omega_i$ by equation (A.21).

If the case of a discrete directional spectrum, the wave amplitude is calculated directly from the spectrum:

$$\tilde{a}_i = \sqrt{E(\omega_i, \theta_i)}. \tag{A.24}$$

In the case of a continuous directional spectrum $S(\omega, \theta)$, the frequency-angle plane should be first divided by a number of non-overlapping cells with dimensions $\Delta\omega_i \times \Delta\theta_i$ (note that cells are not necessarily of the same size). Then, the wave amplitude is calculated as follows:

$$\tilde{a}_i = \sqrt{S(\omega_i, \theta_i)\Delta\omega_i \Delta\theta_i} \tag{A.25}$$

The random phase $\tilde{\varepsilon}_i$ *is* generated using uniform distribution on the interval (0, 2π).

*This page is intentionally blank*

# Appendix B: Effect of Sea State on Ammunition Performance

The following analysis of ammunition effectiveness assumes that a target can be "killed" by a single round. If this is not the case due to a built-in redundancy, the target should be divided into components such that each component could be "killed" by a single round (two separate engines in the example), and the overall effect is then determined by combining state of components.

Consider a target partially covered from an incoming round by waves. Because of the wave cover effect the target exposed area is usually smaller than the total area of the target, $A_T$:

$$A = \eta\, A_T\,, \tag{B.1}$$

where the coefficient $\eta$ shows which part of the target is exposed (not covered by waves). Value of $\eta$ varies between 0 and 1: value $\eta$ = 0 corresponds to entirely hidden (covered) target and value $\eta$ = 1 corresponds to entirely exposed target.

The probability of target kill by an incoming round, $P_k'$, is expressed as follows:

$$P_k' = \mu\, P_k\,, \tag{B.2}$$

where $P_k$ is the baseline probability of kill in the absence of cover (no waves), and $\mu$ is the ammunition effectiveness coefficient showing reduction in ammunition effectiveness due to wave cover.

## B.1 Armour-Piercing and Point-Detonation High-Explosive Rounds

For armour-piercing (AP) and point-detonation high-explosive (PD-HE) rounds probability of a target kill or incapacitation in a single shot is usually expressed as follows:

$$P_k = P_h P_{k|h}\,, \tag{B.3}$$

where $P_k$ is the probability of kill, $P_h$ is probability of round hitting the target, and $P_{k|h}$ is the probability of target kill or incapacitation given a hit.

If shot dispersion in significantly greater than the target area, it can be assumed that the probability of hit is proportional to the target area, as follows:

$$P_h = \rho\, A\,, \tag{B.4}$$

where $\rho$ is the fire density, measured in rounds per square metre, and $A$ is the target exposed area.

Equation (B.3) for $P_k$ can be rewritten with the help of Equations (B.1) and (B.4) as follows:

$$P_k = \rho\, A\, P_{k|h},$$
$$P_k = \rho \frac{A}{A_T} A_T P_{k|h},$$
$$P_k = \rho\, A_T \left(\eta\, P_{k|h}\right),$$
$$P_k = P_h P'_{k|h},$$

where

$$P'_{k|h} = \eta\, P_{k|h} \tag{B.5}$$

stands for reduced probability of kill or incapacitation given a hit.

Therefore, the ammunition effectiveness coefficient is equal to the ratio of exposed target area and the total target area:

$$\mu = \eta. \tag{B.6}$$

## B.2 Air-Burst Munitions

The case of air-bursting fragmenting munitions (ABM) require a special treatment because their effect on a target is due to multiple hits of fragments or pellets as opposed to a single hit from AP and PD-HE rounds.

A qualitative treatment of the problem is presented here; it highlights the significant difference in the effectiveness coefficient between ABM rounds on one side, and AP and PD-HE rounds on the other side. The analytical result, however, is not exact, and the numerical values of the coefficient should be obtained by a detailed numerical analysis of fragment cloud impact on the partially covered target.

Assume that probability of target kill by a single fragment is $p$, and probability of survival of a single fragment hit is $q$:

$$p + q = 1 \tag{B.7}$$

The expected number of fragments hitting the target is proportional to the target exposed area $A$:

$$n = \rho\, A. \tag{B.8}$$

Equation (B.8) can be rewritten with the help of Equation (B.1) as follows:

$$n = \rho\, A_T \frac{A}{A_T},$$

$$n = \eta N , \tag{B.9}$$

where $\rho$ is the fragment cloud density, measured in fragments per square metre, and $N = \rho A_T$ is the number of fragments hitting a fully exposed target. Note that both $n$ and $N$ are, in fact, random numbers; for simplicity it is assumed here that these numbers are deterministic (not random).

Probability of kill of the covered target is calculated as follows:

$$P_k' = 1- q^n, \tag{B.10}$$

and probability of kill of the fully exposed target is:

$$P_k = 1- q^N. \tag{B.11}$$

Equation (B.2) can be derived by combining Equations (B.7), (B.8), (B.10), and (B.11), as follows:

$$P_k ' = \mu P_k,$$

where

$$\mu = \frac{1-(1-p)^{\eta \rho A_T}}{1-(1-p)^{\rho A_T}} \tag{B.12}$$

is the ammunition effectiveness coefficient which shows reduction in ammunition effectiveness due to wave cover.

Therefore, for ABM rounds the ammunition effectiveness coefficient depends on the individual fragment lethality $p$, fragment density $\rho$, and target exposure coefficient $\eta$.

*This page is intentionally blank*

# Appendix C: Frequency Distributions of Wave Cover

*Table C.1. Frequency of particular wave cover values observation, 1.25 m waves*

| Wave cover, m | Angle of fall, degrees | | | | |
|---|---|---|---|---|---|
| | 0 | 2 | 4 | 6 | 8 |
| 0.0 | 0.0014 | 0.4678 | 0.8083 | 0.9498 | 0.9890 |
| 0.1 | 0.0134 | 0.3034 | 0.1483 | 0.0448 | 0.0101 |
| 0.2 | 0.0291 | 0.1133 | 0.0287 | 0.0044 | 0.0006 |
| 0.3 | 0.0454 | 0.0563 | 0.0101 | 0.0005 | 0.0003 |
| 0.4 | 0.0683 | 0.0284 | 0.0031 | 0.0003 | 0.0000 |
| 0.5 | 0.0900 | 0.0162 | 0.0012 | 0.0002 | 0.0000 |
| 0.6 | 0.1030 | 0.0081 | 0.0003 | 0.0000 | 0.0000 |
| 0.7 | 0.1124 | 0.0034 | 0.0000 | 0.0000 | 0.0000 |
| 0.8 | 0.1191 | 0.0019 | 0.0000 | 0.0000 | 0.0000 |
| 0.9 | 0.1082 | 0.0007 | 0.0000 | 0.0000 | 0.0000 |
| 1.0 | 0.0954 | 0.0004 | 0.0000 | 0.0000 | 0.0000 |
| 1.1 | 0.0780 | 0.0001 | 0.0000 | 0.0000 | 0.0000 |
| 1.2 | 0.0560 | 0.0000 | 0.0000 | 0.0000 | 0.0000 |
| 1.3 | 0.0366 | 0.0000 | 0.0000 | 0.0000 | 0.0000 |
| 1.4 | 0.0221 | 0.0000 | 0.0000 | 0.0000 | 0.0000 |
| 1.5 | 0.0113 | 0.0000 | 0.0000 | 0.0000 | 0.0000 |
| 1.6 | 0.0048 | 0.0000 | 0.0000 | 0.0000 | 0.0000 |
| 1.7 | 0.0024 | 0.0000 | 0.0000 | 0.0000 | 0.0000 |
| 1.8 | 0.0016 | 0.0000 | 0.0000 | 0.0000 | 0.0000 |
| 1.9 | 0.0007 | 0.0000 | 0.0000 | 0.0000 | 0.0000 |
| 2.0 | 0.0005 | 0.0000 | 0.0000 | 0.0000 | 0.0000 |
| 2.1 | 0.0002 | 0.0000 | 0.0000 | 0.0000 | 0.0000 |
| 2.2 | 0.0001 | 0.0000 | 0.0000 | 0.0000 | 0.0000 |

*Table C.2. Frequency of particular wave cover values observation, 2.5 m waves*

| Wave cover, m | Angle of fall, degrees | | | | |
|---|---|---|---|---|---|
| | 0 | 2 | 4 | 6 | 8 |
| 0.0 | 0.0012 | 0.2008 | 0.4230 | 0.6339 | 0.7961 |
| 0.1 | 0.0066 | 0.2053 | 0.2681 | 0.2234 | 0.1427 |
| 0.2 | 0.0108 | 0.1413 | 0.1168 | 0.0681 | 0.0335 |
| 0.3 | 0.0145 | 0.1020 | 0.0661 | 0.0313 | 0.0138 |
| 0.4 | 0.0183 | 0.0794 | 0.0419 | 0.0172 | 0.0073 |
| 0.5 | 0.0214 | 0.0595 | 0.0271 | 0.0102 | 0.0033 |
| 0.6 | 0.0257 | 0.0508 | 0.0170 | 0.0066 | 0.0013 |
| 0.7 | 0.0312 | 0.0392 | 0.0118 | 0.0040 | 0.0012 |
| 0.8 | 0.0367 | 0.0311 | 0.0100 | 0.0021 | 0.0005 |
| 0.9 | 0.0434 | 0.0227 | 0.0064 | 0.0014 | 0.0002 |
| 1.0 | 0.0475 | 0.0178 | 0.0045 | 0.0013 | 0.0001 |
| 1.1 | 0.0501 | 0.0135 | 0.0024 | 0.0006 | 0.0000 |
| 1.2 | 0.0514 | 0.0105 | 0.0017 | 0.0003 | 0.0000 |
| 1.3 | 0.0543 | 0.0085 | 0.0013 | 0.0000 | 0.0000 |
| 1.4 | 0.0589 | 0.0058 | 0.0007 | 0.0000 | 0.0000 |
| 1.5 | 0.0558 | 0.0045 | 0.0007 | 0.0000 | 0.0000 |
| 1.6 | 0.0567 | 0.0028 | 0.0001 | 0.0000 | 0.0000 |
| 1.7 | 0.0576 | 0.0012 | 0.0002 | 0.0000 | 0.0000 |
| 1.8 | 0.0520 | 0.0009 | 0.0002 | 0.0000 | 0.0000 |
| 1.9 | 0.0479 | 0.0005 | 0.0000 | 0.0000 | 0.0000 |
| 2.0 | 0.0428 | 0.0006 | 0.0000 | 0.0000 | 0.0000 |
| 2.1 | 0.0406 | 0.0004 | 0.0000 | 0.0000 | 0.0000 |
| 2.2 | 0.0366 | 0.0003 | 0.0000 | 0.0000 | 0.0000 |
| 2.3 | 0.0294 | 0.0003 | 0.0000 | 0.0000 | 0.0000 |
| 2.4 | 0.0253 | 0.0001 | 0.0000 | 0.0000 | 0.0000 |
| 2.5 | 0.0211 | 0.0002 | 0.0000 | 0.0000 | 0.0000 |
| 2.6 | 0.0157 | 0.0000 | 0.0000 | 0.0000 | 0.0000 |
| 2.7 | 0.0114 | 0.0000 | 0.0000 | 0.0000 | 0.0000 |
| 2.8 | 0.0098 | 0.0000 | 0.0000 | 0.0000 | 0.0000 |
| 2.9 | 0.0072 | 0.0000 | 0.0000 | 0.0000 | 0.0000 |
| 3.0 | 0.0051 | 0.0000 | 0.0000 | 0.0000 | 0.0000 |
| 3.1 | 0.0036 | 0.0000 | 0.0000 | 0.0000 | 0.0000 |
| 3.2 | 0.0028 | 0.0000 | 0.0000 | 0.0000 | 0.0000 |
| 3.3 | 0.0020 | 0.0000 | 0.0000 | 0.0000 | 0.0000 |
| 3.4 | 0.0014 | 0.0000 | 0.0000 | 0.0000 | 0.0000 |
| 3.5 | 0.0032 | 0.0000 | 0.0000 | 0.0000 | 0.0000 |

*Table C.3. Frequency of particular wave cover values observation, 3.0 m waves*

| Wave cover, m | Angle of fall, degrees | | | | |
|---|---|---|---|---|---|
| | 0 | 2 | 4 | 6 | 8 |
| 0.0 | 0.0008 | 0.1595 | 0.3450 | 0.5332 | 0.6949 |
| 0.1 | 0.0058 | 0.1695 | 0.2410 | 0.2416 | 0.1899 |
| 0.2 | 0.0083 | 0.1234 | 0.1345 | 0.0914 | 0.0557 |
| 0.3 | 0.0119 | 0.0996 | 0.0787 | 0.0485 | 0.0247 |
| 0.4 | 0.0145 | 0.0774 | 0.0525 | 0.0282 | 0.0132 |
| 0.5 | 0.0164 | 0.0658 | 0.0391 | 0.0180 | 0.0085 |
| 0.6 | 0.0192 | 0.0533 | 0.0290 | 0.0117 | 0.0050 |
| 0.7 | 0.0205 | 0.0472 | 0.0212 | 0.0093 | 0.0033 |
| 0.8 | 0.0253 | 0.0407 | 0.0141 | 0.0052 | 0.0017 |
| 0.9 | 0.0301 | 0.0329 | 0.0113 | 0.0044 | 0.0012 |
| 1.0 | 0.0330 | 0.0281 | 0.0094 | 0.0029 | 0.0012 |
| 1.1 | 0.0357 | 0.0207 | 0.0068 | 0.0019 | 0.0005 |
| 1.2 | 0.0406 | 0.0184 | 0.0054 | 0.0011 | 0.0002 |
| 1.3 | 0.0404 | 0.0153 | 0.0039 | 0.0011 | 0.0000 |
| 1.4 | 0.0432 | 0.0111 | 0.0024 | 0.0008 | 0.0000 |
| 1.5 | 0.0450 | 0.0091 | 0.0016 | 0.0003 | 0.0000 |
| 1.6 | 0.0465 | 0.0073 | 0.0013 | 0.0003 | 0.0000 |
| 1.7 | 0.0475 | 0.0061 | 0.0007 | 0.0001 | 0.0000 |
| 1.8 | 0.0476 | 0.0045 | 0.0007 | 0.0000 | 0.0000 |
| 1.9 | 0.0464 | 0.0031 | 0.0004 | 0.0000 | 0.0000 |
| 2.0 | 0.0477 | 0.0020 | 0.0003 | 0.0000 | 0.0000 |
| 2.1 | 0.0463 | 0.0016 | 0.0001 | 0.0000 | 0.0000 |
| 2.2 | 0.0407 | 0.0006 | 0.0002 | 0.0000 | 0.0000 |
| 2.3 | 0.0371 | 0.0005 | 0.0003 | 0.0000 | 0.0000 |
| 2.4 | 0.0363 | 0.0005 | 0.0001 | 0.0000 | 0.0000 |
| 2.5 | 0.0324 | 0.0004 | 0.0000 | 0.0000 | 0.0000 |
| 2.6 | 0.0315 | 0.0003 | 0.0000 | 0.0000 | 0.0000 |
| 2.7 | 0.0250 | 0.0003 | 0.0000 | 0.0000 | 0.0000 |
| 2.8 | 0.0235 | 0.0002 | 0.0000 | 0.0000 | 0.0000 |
| 2.9 | 0.0198 | 0.0002 | 0.0000 | 0.0000 | 0.0000 |
| 3.0 | 0.0168 | 0.0002 | 0.0000 | 0.0000 | 0.0000 |
| 3.1 | 0.0135 | 0.0002 | 0.0000 | 0.0000 | 0.0000 |
| 3.2 | 0.0107 | 0.0000 | 0.0000 | 0.0000 | 0.0000 |
| 3.3 | 0.0092 | 0.0000 | 0.0000 | 0.0000 | 0.0000 |
| 3.4 | 0.0069 | 0.0000 | 0.0000 | 0.0000 | 0.0000 |
| 3.5 | 0.0053 | 0.0000 | 0.0000 | 0.0000 | 0.0000 |
| 3.6 | 0.0040 | 0.0000 | 0.0000 | 0.0000 | 0.0000 |
| 3.7 | 0.0040 | 0.0000 | 0.0000 | 0.0000 | 0.0000 |
| 3.8 | 0.0027 | 0.0000 | 0.0000 | 0.0000 | 0.0000 |
| 3.9 | 0.0023 | 0.0000 | 0.0000 | 0.0000 | 0.0000 |
| 4.0 | 0.0056 | 0.0000 | 0.0000 | 0.0000 | 0.0000 |

**DEFENCE SCIENCE AND TECHNOLOGY ORGANISATION**
**DOCUMENT CONTROL DATA**

1. PRIVACY MARKING/CAVEAT (OF DOCUMENT)

2. TITLE

Probabilistic Model of a Floating Target Behaviour in Rough Seas

3. SECURITY CLASSIFICATION (FOR UNCLASSIFIED REPORTS THAT ARE LIMITED RELEASE USE (L) NEXT TO DOCUMENT CLASSIFICATION)

| | |
|---|---|
| Document | (U) |
| Title | (U) |
| Abstract | (U) |

4. AUTHOR(S)

Rada Pushkarova

5. CORPORATE AUTHOR

DSTO Defence Science and Technology Organisation
PO Box 1500
Edinburgh South Australia 5111 Australia

| 6a. DSTO NUMBER | 6b. AR NUMBER | 6c. TYPE OF REPORT | 7. DOCUMENT DATE |
|---|---|---|---|
| DSTO-TN-1196 | AR-015-679 | Technical Note | July 2013 |

| 8. FILE NUMBER | 9. TASK NUMBER | 10. TASK SPONSOR | 11. NO. OF PAGES | 12. NO. OF REFERENCES |
|---|---|---|---|---|
| 2012/1235913/1 | 07/021 | COMWAR | 33 | 14 |

13. DSTO Publications Repository

http://dspace.dsto.defence.gov.au/dspace/

14. RELEASE AUTHORITY

Chief, Maritime Division

15. SECONDARY RELEASE STATEMENT OF THIS DOCUMENT

*Approved for public release*

OVERSEAS ENQUIRIES OUTSIDE STATED LIMITATIONS SHOULD BE REFERRED THROUGH DOCUMENT EXCHANGE, PO BOX 1500, EDINBURGH, SA 5111

16. DELIBERATE ANNOUNCEMENT

No Limitations

17. CITATION IN OTHER DOCUMENTS Yes

18. DSTO RESEARCH LIBRARY THESAURUS

Sea surface, Probabilistic Modelling, Gunnery

19. ABSTRACT

This note presents the results from modelling of floating target visibility and wave cover in rough seas. Waves on the sea surface can hide a target from observer's view affecting aiming and ammunition effectiveness. The randomly moving sea surface was modelled using a double peaked wave spectrum. The moving sea surface model was used to estimate height of an object hidden by waves depending on angle of sight, wave direction, significant wave height, target speed and time. Based on this data wave cover frequency distributions were calculated. A possible method of using this data in naval gun performance analysis for armour-piercing, point detonation high explosive, and air burst rounds was suggested.